A heuristic approach to effective sensor placement for modeling of a cylinder wake

Article *in* Computers & Fluids · January 2006

DOI: 10.1016/j.compfluid.2004.11.002

3 authors, including:

Kelly Cohen
University of Cincinnati
214 PUBLICATIONS **1,035** CITATIONS
SEE PROFILE

Stefan Siegel
Atargis Energy Corporation
108 PUBLICATIONS **869** CITATIONS
SEE PROFILE

Available online at www.sciencedirect.com
SCIENCE DIRECT®
Computers & Fluids 35 (2006) 103–120
computers & fluids
www.elsevier.com/locate/compfluid

A heuristic approach to effective sensor placement for modeling of a cylinder wake

Kelly Cohen, Stefan Siegel *, Thomas McLaughlin

Department of Aeronautics, 2354 Fairchild Drive Suite 6H27, US Air Force Academy, CO 80840-6222, USA

Received 13 August 2003; received in revised form 7 September 2004; accepted 2 November 2004
Available online 23 February 2005

Abstract

The effectiveness of a sensor configuration for feedback flow control on the wake of a circular cylinder is investigated in both direct numerical simulation as well as in a water tunnel experiment. The research program is aimed at suppressing the von Kármán vortex street in the wake of a cylinder at a Reynolds number of 100. The design of sensor number and placement was based on data from a laminar two-dimensional simulation of the Navier–Stokes equations for the unforced condition. A low-dimensional proper orthogonal decomposition (POD) was applied to the vorticity calculated from the flow field and sensor placement was based on the intensity of the resulting spatial eigenfunctions. The numerically generated data was comprised of 70 snapshots taken over three cycles from the steady state regime. A linear stochastic estimator (LSE) was employed to map the velocity data to the temporal coefficients of the reduced order model. The capability of the sensor configuration to provide accurate estimates of the four low-dimensional states was validated experimentally in a water tunnel at a Reynolds number of 108. For the experimental wake, a sample of 200 particle image velocimetry (PIV) measurements was used. Results show that for experimental data, the root mean square estimation error of the estimates of the first two modes was within 6% of the desired values and for the next two modes was within 20% of the desired values. This level of error is acceptable for a moderately robust controller.

* Corresponding author. Tel.: +1 719 333 9080; fax: +1 719 333 4813.
E-mail address: Stefan.Siegel@usafa.af.mil (S. Siegel).

0045-7930/$ - see front matter © 2005 Elsevier Ltd. All rights reserved.
doi:10.1016/j.compfluid.2004.11.002

Nomenclature

$a_n(t)$	time dependent coefficient, of nth mode, of the low-dimensional model
b_n	coefficients associated with the control input, of nth mode, of low-dimensional model
C_s^n	coefficients of the linear stochastic estimator
C_d	mean drag coefficient, $C_\mathrm{d} = F_D/5\rho U_\infty^2 \cdot D \cdot 1$
D	cylinder diameter
f	vortex shedding frequency
f_a	feedback control input to the cylinder
F_D	drag force
g_k	quadratic nonlinear function used in low-dimensional, time-depending model
Re	Reynolds number, $Re = U_\infty D/\upsilon$
St	Strouhal number, $St = D/U_\infty$
u_s	sensor measurement of stream-wise velocity
$\tilde{\omega}(x,y,t)$	total vorticity field
$\Omega(x,y)$	mean vorticity distribution
U_∞	freestream velocity
$\omega(x,y,t)$	fluctuating vorticity component
x, y	spatial coordinates
α	skew angle of attack of the incoming flow used to trigger CFD simulation
$\phi(x,y)$	spatial eigenfunction
υ	kinematic viscosity

1. Introduction

One of the main purposes of flow control is the improvement of aerodynamic characteristics of air vehicles and munitions enabling augmented mission performance. An important area of flow control research involves the phenomenon of vortex shedding behind bluff bodies. These bodies often serve some vital operational function. Their purpose is not to augment aerodynamic efficiency and often aerodynamic performance is sacrificed for functionality. Flow separates from large sections of the bluff body's surface. The resulting wake behind the bluff body, known as a vortex street, exhibits vortex shedding which leads to a sharp rise in drag, noise and fluid-induced vibration [1]. The ability to control the wake of a bluff body could be used to reduce drag, increase mixing and heat transfer, and enhance combustion [2–4].

Shedding of counter-rotating vortices is observed in the wake of a two-dimensional cylinder above a critical Reynolds number ($Re \sim 47$, non-dimensionalized with respect to freestream speed and cylinder diameter). This phenomenon is often referred to as the von Kármán vortex street [2]. Fig. 1, a picture taken at the center line of an unforced cylinder wake at the USAF Academy's water tunnel, shows the von Kármán vortex street at $Re = 120$. The flow is from left to right.

Drag, noise and vibration reduction are possible by controlling the wake of a bluff body. The flow may be influenced using several different forcing techniques and the wake response is similar for different types of forcing [1]. The following forcing methods have been employed: acoustic

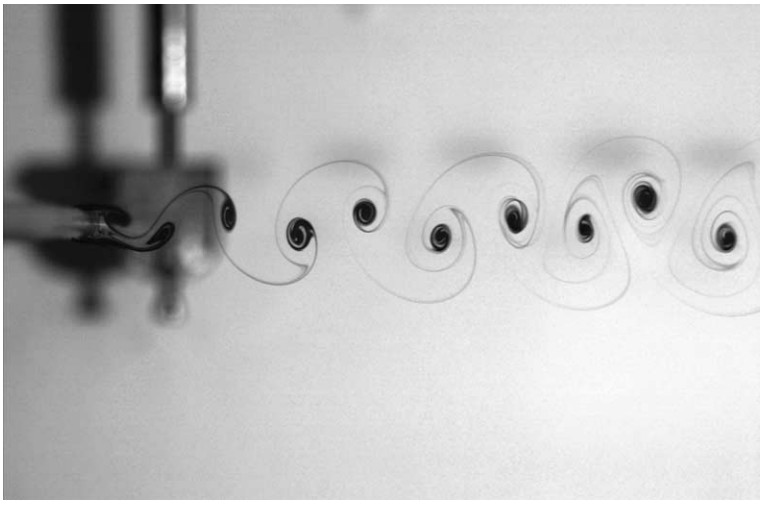

Fig. 1. Circular cylinder wake (Re = 120, diameter D = 3.97 mm, U_∞ = 30 mm/s, water flow visualization).

excitation of the wake, longitudinal, lateral or rotational vibration of the cylinder, and alternate blowing and suction at separation points [1].

The Reynolds regime studied in this effort corresponds to the low Reynolds number, laminar, two-dimensional cylinder wake (the regular range persists up to $Re \sim 194$ as detailed by Williamson [5]). Beyond this range the nature of the vortex shedding transitions to several three-dimensional regimes with increase in the Reynolds number [5]. When active open loop forcing of the wake is employed, the vortices in the wake can be "locked" at the forcing signal. This also strengthens the vortices and consequently increases the drag. The cylinder wake may be controlled by forcing the flow. Open loop forcing has been successfully employed to delay boundary layer transition [1]. He et al. [6] apply this open-loop forcing approach to the boundary control by rotation of the flow around a cylinder and show up to 60% drag reduction for Reynolds numbers of 200–1000. As opposed to the open-loop approach, in this effort, the unsteady wake is controlled using a feedback controller. Active closed-loop flow control has been found to be an effective means for suppression of self-excited flow oscillations without geometry modification [1].

Three of the popular approaches for feedback control of a two-dimensional wake are direct feedback control, optimal control and control based on low-dimensional modeling of the flow. Direct feedback control involves the introduction of sensors in the wake and uses a simple control law, which produces a command to the actuator that forces the flow. Experimental studies show that a linear proportional feedback control based on a single sensor feedback is able to delay the onset of the wake instability, rendering the wake stable at a Reynolds number about 20% higher than the unforced case (Re = 47). Above Re = 60, a single-sensor feedback may suppress the original mode but destabilizes one of the other modes [4]. Li and Aubry [7] introduce a feedback controller capable of manipulating the flow using transverse displacements with the aim of maintaining zero lift at all times. Direct numerical simulation studies of the flow show that this control algorithm is capable of keeping the lift close to zero in the impulsively started viscous flow and, therefore, controlling vortex shedding [7].

The optimal control approach is more structured as it applies conventional and proven model-based control strategies such as optimal control theory for flow control problems. The central idea here is to minimize a cost function that satisfies the Navier–Stokes equations that govern the flow. For example, Abergel and Temam [8] developed conditions for optimality which minimizes a cost function that represents the drag on a body. The main disadvantage of the optimal control approach is the computational problems associated with the nonlinearities of the cumbersome unsteady Navier–Stokes-equations. To illustrate this issue, Li et al. [9] point out that for a steady-state problem that has N time steps, the dimension of the unsteady problem is N times larger in comparison. This drawback adversely effects real time implementation of optimal flow control and has led to the development of several sub-optimal approaches surveyed by Li et al. [9]. Homescu et al. [10] solve the open-loop optimal control problem that consists of finding the optimal angular velocity of the cylinder such that the Karman vortex shedding in the wake of the cylinder is suppressed.

Low-dimensional modeling is a vital building block when it comes to realizing a structured model-based closed-loop strategy for flow control. For control purposes, a practical procedure is needed to break down the velocity field, governed by Navier–Stokes partial differential equations, by separating space and time. A common method used to substantially reduce the order of the model is proper orthogonal decomposition (POD). This method is an optimal approach in that it will capture a larger amount of the flow energy in the fewest modes of any decomposition of the flow. The two-dimensional POD method was used to identify the characteristic features, or modes, of a cylinder wake as demonstrated by Gillies [1].

The major building blocks of this structured approach are comprised of a reduced order POD model, a state estimator and a controller. The desired POD model contains an adequate number of modes to enable reasonable modeling of the temporal and spatial characteristics of the large scale coherent structures inherent in the flow though it may not faithfully reproduce the flow. A POD procedure may be used to derive a set of reduced order ordinary differential equations by projecting the Navier–Stokes equations onto the modes. Further details of the POD method may be found in the book by Holmes et al. [11]. A common approach referred to as the method of "snapshots" introduced by Sirovich [12] is employed to generate the basis functions of the POD spatial modes from flow-field information obtained using either experiments or numerical simulations. This approach to controlling the global wake behavior behind a circular cylinder was effectively employed by Gillies [1] and is also the approach followed in this research effort.

For low-dimensional control schemes to be implemented, a real-time *estimation* of the modes present in the wake is necessary, since it is not possible to measure them directly, especially in real-time. An illustration of the various blocks within the low-dimensional modeling approach is presented in Fig. 2. Velocity field data, provided from either simulation or experiment, is fed into the POD procedure. The time histories of the temporal coefficients of the POD model are determined by applying the least squares technique to the spatial eigenfunctions and the unforced flow. Then, the estimation of the low-dimensional states is provided using a linear stochastic estimator (LSE). Sensor measurements may take the form of wake velocity measurements, as in this effort, or for an application based on surface-mounted pressure measurements and/or shear stress sensors. This process leads to the state and measurement equations, required for design of the control system. For practical applications it is desirable to reduce the information required for estimation to the minimum.

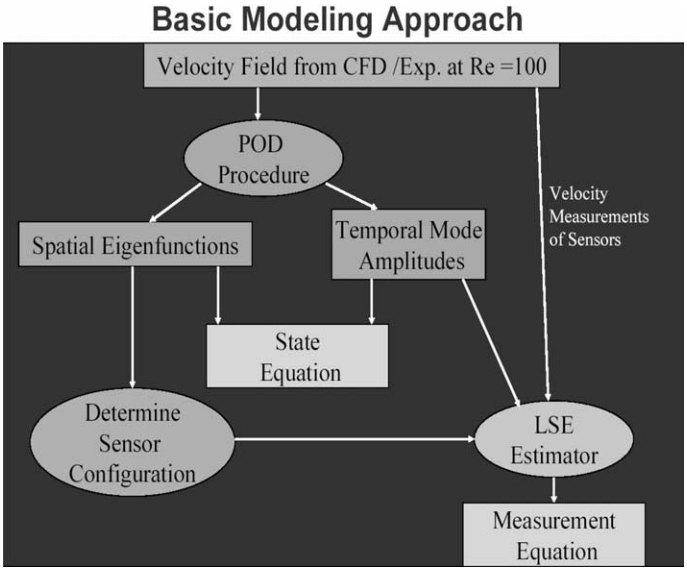

Fig. 2. Low-dimensional modeling strategy.

The requirement for the estimation scheme then is to behave as a modal filter that "combs out" the higher modes. The main aim of this approach is to thereby circumvent the destabilizing effects of observation "spillover" as described by Balas [13]. Spillover has been the cause for instability in the control of flexible structures and modal filtering was found to be an effective remedy [14]. The intention of the proposed strategy is that the signals, provided by a certain configuration of sensors placed in the wake, are processed by the estimator to provide the estimates of the first two modes. The estimation scheme, based on the linear stochastic estimation procedure introduced by Adrian [15], predicts the temporal amplitudes of the first two POD modes from a finite set of measurements obtained from either computational or experimental data. The linear stochastic estimation of POD modes was successfully implemented by Cohen et al. [16] for control of the Ginzburg–Landau wake model. A major design challenge lies in finding an appropriate number of sensors and their locations that will best enable the desired modal filtering. The need for modal filtering and the search for suitable sensor configurations is a problem common to the control of flexible structures, where a considerable amount of work has been done [17,18] and can be leveraged. Meirovitch [14] provides a survey of some effective strategies.

Section 2 describes the research objective and the uniqueness of the developed approach. The direct numerical simulation of the Navier–Stokes equations, using the computational fluid dynamic (CFD) solver COBALT is described and presented in Section 3. This is followed in Section 4 by the development of the low-dimensional POD model based on the vorticity in the flow-field. Then, in Section 5, based on the POD model, a sensor configuration is developed to estimate the first four low-dimensional vorticity states. The sensor configuration design will be based on CFD data. Section 6 describes the experimental setup and the above sensor configuration design is validated. Finally, Section 7 summarizes the conclusions of this research and provides some recommendations for future work.

2. Research objective

Recent research on closed-loop control of the wake instabilities by Park et al. [3] has addressed the issue of sensor placement and number. The method used has been based on trial-and-error with a new search cycle required for each Reynolds number. This approach is tedious and it is important to develop simple and effective heuristics for sensor placement and number based on the vorticity flow field. The main objective of this research effort is to demonstrate and experimentally validate a systematic approach, based on the spatial eigenfunctions of the POD model, for determining sensor number and location for real-time estimation of the truncated POD states of a cylinder wake. This method does not need any additional computational effort beyond the development of the low-dimensional POD model. Hence, the computational cost is one of the major benefits of the proposed approach. It is imperative to note that the scope of this paper does not include control law development and closed-loop control studies.

3. Computational model

A simple model of the flow-field was sought to design sensor configurations for feedback control algorithms. The model primarily needs to accurately capture the dynamic behavior of the flow field and this need to be verified with experimental data presented in the literature. Numerical simulations were conducted on Cobalt Solutions COBALT [19] solver V.2.02. In this effort, the above solver was used for direct numerical solution of the Navier–Stokes equations with second order accuracy in time and space. An unstructured two-dimensional grid with 63 700 nodes and 31 752 elements was used. The grid extended from −16.9 cylinder diameters to 21.1 cylinder diameters in the x (streamwise) direction, and ±19.4 cylinder diameters in y (flow normal) direction. Additional simulation parameters are as follows:

- two-dimensional cylinder, diameter = 1 m,
- Reynolds number (Re) = 100 (ideal gas),
- laminar Navier–Stokes equations,
- vortex shedding frequency—5.55 Hz,
- mean flow, $U = 34$ m/s,
- damping coefficients: advection = 0.01; diffusion = 0.00,
- 32 iterations for matrix solution scheme,
- 3 Newtonian sub-iterations,
- non-dimensional time step, $\Delta t^* = \Delta t \cdot U/D = 0.05$,
- time step, $\Delta t = 0.00147$ s.

The simulation was triggered by skewing the incoming mean flow by $\alpha = 0.5°$ to introduce an initial perturbation. An important issue concerning the validity of the CFD model needs to be addressed before using the data. For validation of the unforced cylinder wake CFD model at $Re = 100$, the resulting value of the mean drag coefficient, C_d, will be compared to experimental and computational investigations reported in the literature. At $Re = 100$, experimental data, reported by Oertel [20] and Panton [21] point to C_d values from 1.26 to 1.4. Furthermore, Min

and Choi [22] report on several numerical studies that obtained drag coefficients of 1.35 and 1.337. The COBALT CFD model, used in this effort results in a $C_d = 1.35$ at $Re = 100$, which compares well with the reported literature. Another important benchmark parameter concerns the value of the non-dimensional Strouhal number (St) for the unforced cylinder wake. Experimental results at $Re = 100$, presented by Williamson [5], point to St values of 0.167–0.168. The COBALT CFD model, used in this effort, has a $St = 0.163$ at $Re = 100$ which also compares well with the reported literature.

4. POD modeling

Feasible real-time estimation and control of the cylinder wake may be effectively realized by reducing the model complexity of the cylinder wake as described by the Navier–Stokes equations, using POD techniques. POD, a non-linear model reduction approach is referred to in the literature as the Karhunen–Loeve expansion [11]. The truncated POD model will contain an adequate number of modes to enable modeling of the temporal and spatial characteristics of the large-scale coherent structures inherent in the flow, but no more modes than necessary.

In this effort, the basis functions of the POD spatial modes are obtained from the numerical solution of the Navier–Stokes equations using the COBALT CFD simulation program [19]. In all, 70 snap-shots, equally spaced at 0.00735 s apart, were used. The time between snapshots is five times the simulation time step. The snap-shots were taken after ensuring that the cylinder wake reached steady state. Only the vorticity, obtained from the experiment/CFD flow field data was used for the sensor placement and number studies reported in this effort. For control design purposes, the POD method enables the Navier–Stokes equations to be modeled as a set of ordinary differential equations (ODE) [23]. The general decomposition of on a scalar vorticity field is as follows:

$$\tilde{\omega}(x, y, t) = \Omega(x, y) + \omega(x, y, t) \tag{1}$$

where Ω [s^{-1}] denotes the mean vorticity and ω [s^{-1}] is the fluctuating component. In the present investigation, we chose to use vorticity as the data basis. This reduces the POD procedure to a scalar operation in a two-dimensional flow field, while capturing the most dominant features of the flow. This fluctuating vorticity field may then be expanded as:

$$\omega(x, y, t) = \sum_{k=1}^{n} a_k(t)\phi_i^{(k)}(x, y) \tag{2}$$

where $\phi_i(x,y)$ represents the non-dimensional spatial eigenfunctions (see Fig. 3) and $a_k(t)$ denotes the time-dependent coefficients having units of s^{-1} (see Fig. 4) determined from the POD procedure. Eq. (2) may be applied to the velocity components u and v, or it may be used to decompose vorticity as it does in this paper. A decision needs to be taken concerning which of the above values are required for effective feedback. In a recent paper, Cameron et al. [24] use the u component of the velocity in the POD model. In this effort, vorticity is used.

Next, the empirical correlation matrix, R is computed. A simple approximation technique is applied to obtain the numerical integration. In this effort, the correlation matrix is computed using

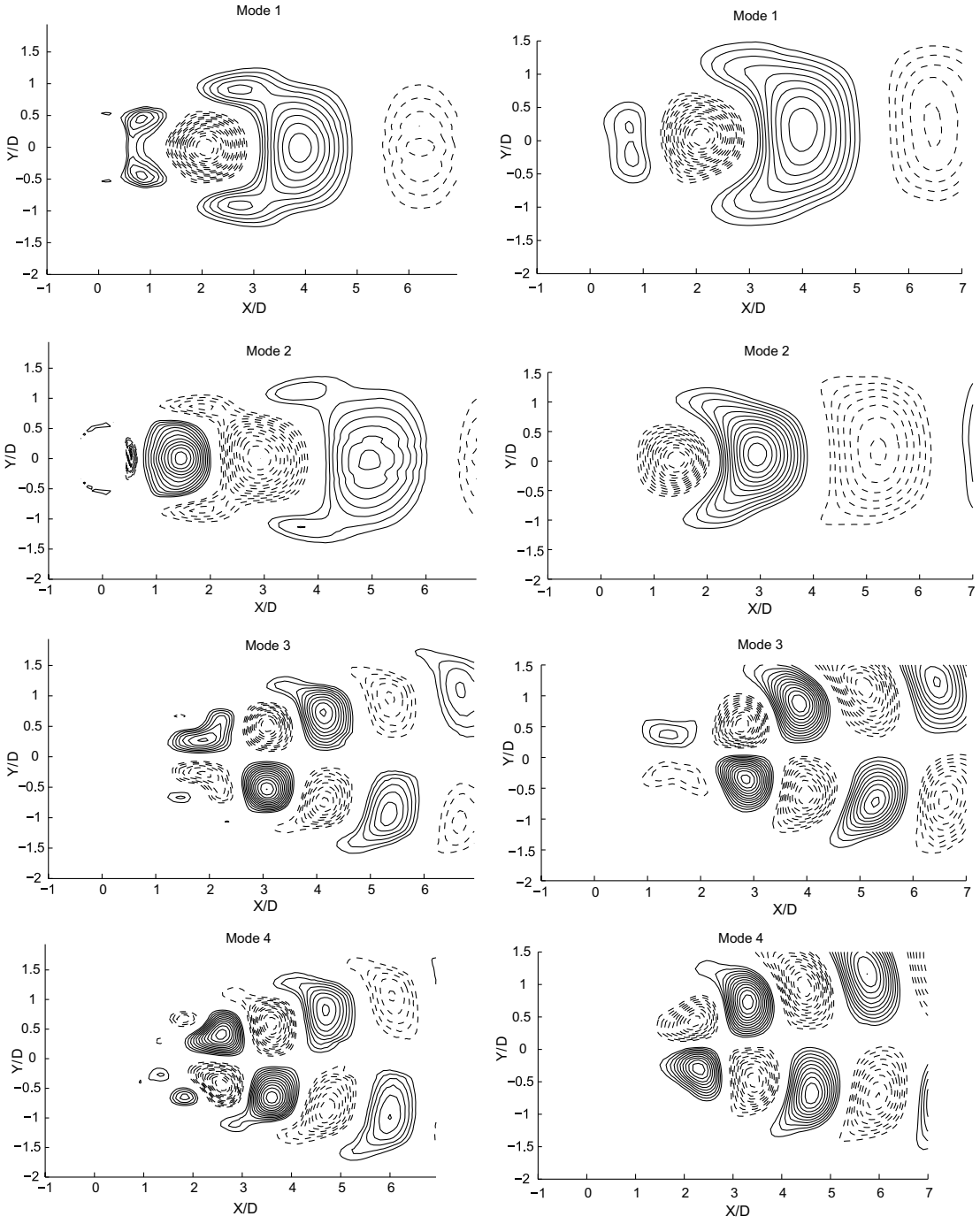

Fig. 3. Spatial vorticity eigenfunctions of 4 mode model. The left column contains the eigenfunctions obtained from CFD data at $Re = 100$, and the right column contains the eigenfunctions obtained from experimental data at $Re = 108$. Solid lines are positive, dashed lines are negative isocontours.

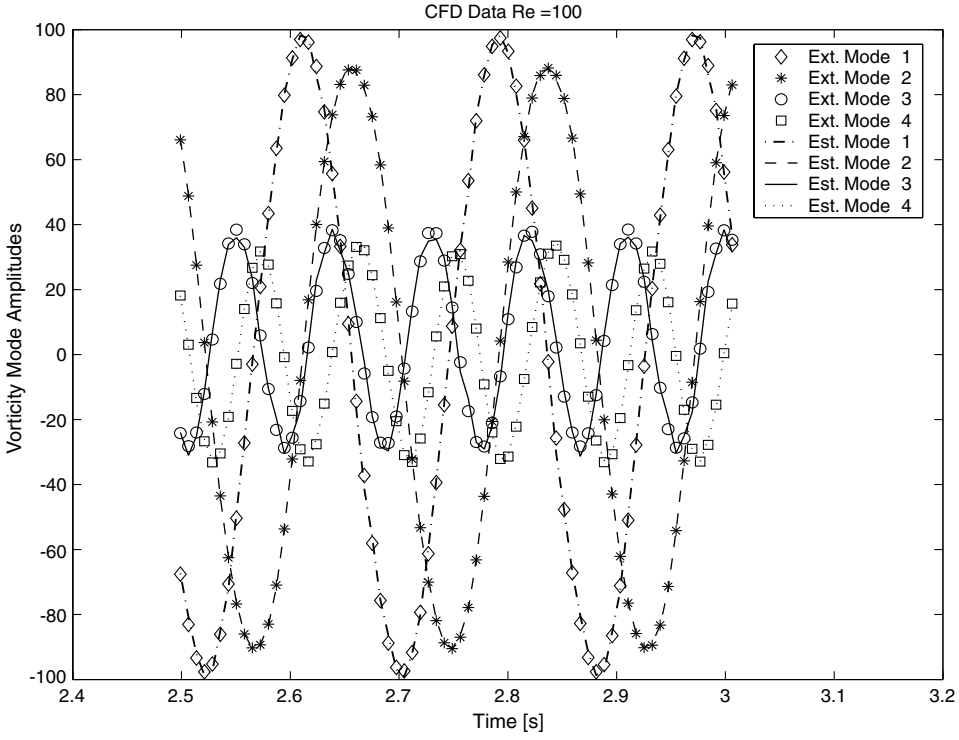

Fig. 4. Extracted mode amplitudes projected on the estimated ones for CFD data at $Re = 100$.

the inner product [23]. Solving the eigenvalue problem, the eigenvalues and the orthogonal spatial eigenfunctions, $\phi_i(x,y)$ are obtained (see Fig. 3). Since the eigenvalues measure the relative energy of the system dynamics contained in that particular mode, they may be normalized to correspond to a percentage. Finally, the time histories of the temporal coefficients of the POD model, $a_k(t)$, are determined using the extracted spatial modes and the data of the unforced flow. For an arbitrarily forced circular cylinder, we can write the low-dimensional wake model [25] as:

$$\frac{da_k}{dt} = g_k(a_n) + b_k f_a \tag{3}$$

where g_k, for k modes, is a quadratic non-linear function of the time-dependent mode coefficients. The coefficients associated with the control input are b_k and f_a is the feedback control input to the cylinder. For the open-loop case $f_a = 0$. For a full state feedback system, the closed-loop control input, f_a, is a function of a_k. However, it is not possible to obtain a direct measurement of a_k. The POD algorithms, based on the above steps and realized in MATLAB®, were applied to the CFD and experimental data obtained at $Re = 100$ and $Re = 108$ respectively. The "energy" content for the first eight vorticity modes is presented in Table 1. It can be seen that most of this "energy" of the flow lies in the first eight modes. An important aspect of reduced order modeling concerns truncation. How many modes are important and what criteria could be implemented for effective truncation?

Table 1
Energy content (eigenvalues) for the first eight vorticity modes of the POD model (%)

	Mode I	Mode II	Mode III	Mode IV	Mode V	Mode VI	Mode VII	Mode VIII
CFD data $Re = 100$	46.17	37.82	5.47	4.94	2.31	2.26	0.35	0.34
Experimental data $Re = 108$	43.40	41.98	3.03	2.73	0.79	0.70	0.35	0.30

The answers to the above questions have been addressed by Cohen et al. [25]. This effort showed that control of the POD model of the von Kármán vortex street in the wake of a circular cylinder at $Re = 100$ is enabled using just the first mode. Furthermore, feedback based on the first mode alone suppressed all the other modes in the four mode POD model. In view of this result, truncation of the POD model will take place after the first four modes, which contain 94.4% of the total amount of "energy". At this point, it is imperative to note the difference between the number of modes required to *reconstruct* the flow and the number of modes required for effective low-dimensional modeling for control design. In this effort, we are interested in estimating only those modes required for closed-loop control. On the other hand, an accurate reconstruction of the velocity field based on a low-dimensional model may be obtained using between 4 and 8 modes [23]. The POD algorithm was applied to the vorticity in the flow as described in Eq. (1). The velocity field may be obtained from a CFD simulation or from a real-time PIV (particle image velocimetry) system as described by Siegel et al. [26]. The quintessential question is whether an effective estimate of the states, of the 4 mode low-dimensional model, a_k, can be estimated based on the real-time velocity field measurements. The next section addresses the details that provides the estimate of the first four modes, a_1–a_4.

5. Estimation and sensor configuration

The time histories of the temporal coefficients of the POD model are determined by introducing the spatial eigenfuctions into the flow field data using the least squares technique. The intent of the proposed strategy is that the velocity measurements provided by the sensors are processed by the estimator to provide the estimates of the first two temporal modes. The estimation scheme, based on the linear stochastic estimation procedure introduced by Adrian [15], predicts the temporal amplitudes of the first four POD modes (about 95% of the kinetic energy) from a finite set of velocity measurements obtained from the CFD solution of the uncontrolled cylinder wake. For each sensor configuration, 70 velocity measurements were used equally spaced at 0.00735 s apart. All the measurements were taken after ensuring that the cylinder wake reached steady state. Only data concerning velocity components in the direction of the flow were used for the sensor placement and number studies reported in this effort. The vorticity mode amplitudes, a_1–a_4, presented in Fig. 4 at the above 70 discrete times were mapped onto the extracted sensor signals, u_s, as follows:

$$a_n(t) = \sum_{s=1}^{m} C_s^n u_s(t) \tag{4}$$

where m is the number of sensors and C_s^n represents the coefficients of the linear mapping. The effectiveness of a linear mapping between for velocity measurements and POD states has been experimentally validated by Cameron et al. [24]. The coefficients C_s^n ($n = 1$–4; $s = 1,m$) in Eq. (4) are obtained via the linear stochastic estimation method from the set of discrete sensor signals and temporal mode amplitudes. For the sensor configuration, the effectiveness of the linear stochastic estimation process for the estimation of the first four temporal mode amplitudes, a_1–a_4, is calculated. The extracted mode amplitudes are obtained by introducing the spatial eigenfunctions into the snapshot data of the velocity field using the least squares method. For sake of convenience, this RMS error is normalized with the RMS of the desired extracted mode amplitudes, presented as a percentage. The resulting error percentage and the number of sensors may be integrated together into a cost function and the purpose of the design process would then be to select the configuration that minimizes this cost. Furthermore, Cameron et al. [24] demonstrate the robustness of the developed heuristic approach to slight variations in the value of Reynolds numbers ($82 < Re < 100$).

The issue of sensor placement and number has been dealt with in an ad hoc manner in published studies concerning closed-loop flow control. In this effort, an attempt will be made to emulate some of the proven successes from the field of structural control. Heuristically speaking, when some very fine dust particles are placed on a flexible plate, excited at one of its natural frequencies, after a short while the particles arrange themselves in a certain pattern typical of those frequencies. The particles will be concentrated in the areas that do not experience any motion (the nodes). On the other hand, at the areas where the motion is most active (the internodes) will be clean of particles. It is at the internodes that the vibrational energy of that particular mode is at a maximum and sensors placed at these locations are extremely effective in estimating that particular mode [27].

The above heuristic approach has been used by Bayon de Noyer [27] in locating effective sensor locations for acceleration feedback control to alleviate tail buffeting of a high performance twin tail aircraft. Note the usage of the term "effective sensor configuration" as it is based on validated heuristics as opposed to "optimal sensor configuration" that results from a mathematical pattern search for a sensor configuration. So, what needs to be done to determine an effective sensor configuration is to find the areas of energetic modal activity.

The spatial eigenfunctions obtained from the POD procedure provides information concerning the location of areas where modal activity is at its highest. These energetic areas would be the maxima (solid lines in Fig. 3) and minima (dashed lines in Fig. 3). Note that in the case of modes 2 and 4 the maxima and the minima of the experimentally obtained eigenfunctions have the opposite sign when compared to the eigenfunctions obtained from the CFD data. However, this difference is merely caused by the numerical algorithm and does not affect the similarity. Placing sensors at the energetic maxima and minima of each mode is the basic hypothesis of this effort and the purpose of the CFD simulation is to design a sensor configuration which is later validated using water tunnel experiments. Location of vorticity maxima/minima of the spatial eigenfunctions (see Fig. 3) are used for sensor placement as shown in Table 2. The locations of the sensors in Table 2 are referenced in terms of the coordinates, non-dimensionalized with respect to the cylinder diameter D, namely, X/D and Y/D. A sensor was placed on each the maxima and the minima of modes 1 and 2 (see Fig. 3). On the other hand, for effective estimation, two pairs of sensors each are located on maxima/minima of modes 3 and 4. The estimated versus desired mode amplitude

Table 2
Location of vorticity maxima/minima of the spatial eigenfunctions used for sensor placement

	X/D	*Y/D*
Mode 1		
1	2.0	0.0
2	4.0	0.0
Mode 2		
3	1.5	0.0
4	3.0	0.0
Mode 3		
5	2.2	−0.3
6	2.3	0.3
7	3.3	−0.6
8	3.3	0.6
Mode 4		
5	2.8	0.5
6	2.8	−0.5
7	3.8	0.8
8	3.8	−0.8

Table 3
RMS estimation error from LSE procedure

	Mode 1 (%)	Mode 2 (%)	Mode 3 (%)	Mode 4 (%)
CFD $Re = 100$	2.1	0.6	7.1	2.9
Experiment $Re = 108$	6.0	5.3	22.1	20.3

plot, for the above sensor configuration is presented in Fig. 4. For this configuration, the RMS estimation errors are provided in Table 3.

At this point, it is important to reflect upon a control system attribute referred to as robustness. Robustness is a property which guarantees that the essential functions of the designed systems are maintained under adverse conditions in which the model no longer reflects reality [28]. The description of plant uncertainty, which is the characterization of how the "true" plant might differ from the nominal one, is taken into account during the robust control design process. Considering the fact that the LSE is providing vorticity estimates, the RMS values in Table 3 are low and can be dealt with using a moderately robust controller.

6. Experimental set up and validation

The basis for validation of the design concerning sensor configuration was experimentally obtained from velocity measurements in the wake of a circular cylinder at $Re = 108$. The experimental measurements were obtained in the Eidetic Model 2436 recirculating water tunnel. The water tunnel is situated in the Aeronautics Laboratory at the US Air Force Academy. The cross-section

of the water tunnel is 38 cm × 38 cm and the test section is 1.5 m in length. The circular cylinder model, as depicted in Fig. 5, is comprised of a stainless steel rod, has a diameter, D, of 3.97 mm and a span, L, of 381 mm. The aspect ratio of the cylinder, L/D, is about 95. The cylinder was positioned horizontally in the water tunnel. The actuation system shown in Fig. 5 was not used for the unforced experiments in this effort.

The Reynolds number ($Re = U_\infty D/\upsilon$) is calculated from the freestream velocity, obtained from PIV measurements. The kinematic viscosity, υ, is calculated on the basis of temperature measurements. The natural shedding frequency of the cylinder, f, was calculated from the period of the time dependent mode amplitude, a_1, as shown in Fig. 6. The calculated Strouhal number was then obtained based on the shedding frequency calculation. Williamson [5] provides experimental data that correlates the Reynolds number to the Strouhal number for a circular cylinder and this information is used to obtain the expected Strouhal number. In Table 4, the expected and the calculated Strouhal numbers are compared. Furthermore, an uncertainty analysis provides a Reynolds number accuracy of ±7.5 (or 6–7% error). The superposition of the percent difference presented in Table 4 on the data provided by Williamson [5] validates the experimental working point at a Reynolds number of 108.

The digital PIV system provided two-dimensional velocity field measurements in the wake of the unforced cylinder from which the vorticity was calculated. The field of view extended from the trailing edge of the cylinder to approximately eight diameters ($8D$) downstream. The PIV system employed a 1 Mpixel CCD camera. It was operated in dual exposure mode using cross correlation to determine the pixel displacements based on two snapshots. A 32 × 32 pixel interrogation area with 50% overlap was used in the data reduction. This setup results in vector field of

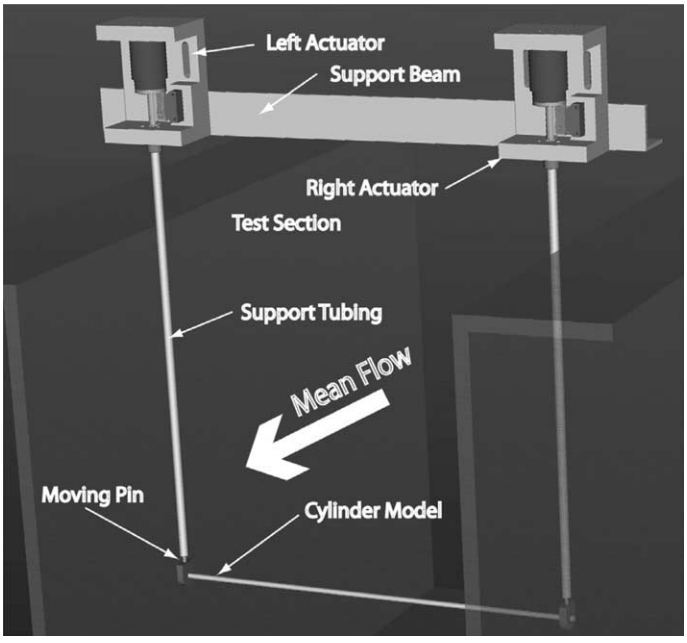

Fig. 5. Experimental circular cylinder model setup at US Air Force Academy.

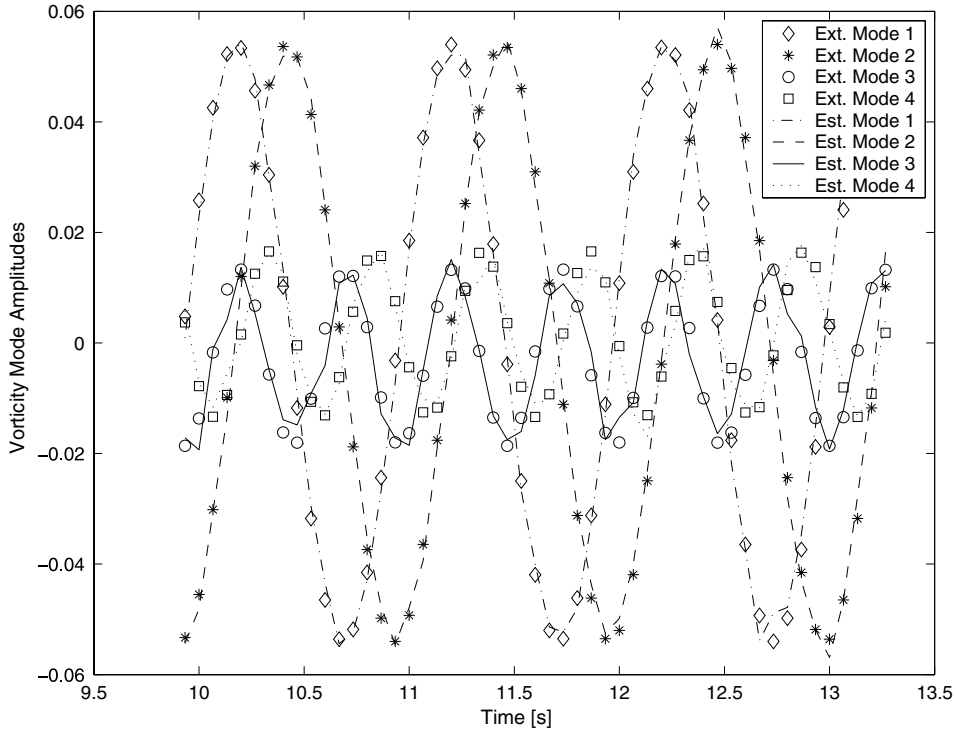

Fig. 6. Extracted mode amplitudes projected on the estimated ones for experimental data at $Re = 108$.

Table 4
Validation of the data (Re vs. St)

	Reynolds number	Expected Strouhal number [18]	Observed Strouhal number	Percent difference (%)
CFD $Re = 100$	100	0.165	0.163	1.2
Experiment $Re = 108$	108	0.168	0.160	4.8

49×49 vectors. The flow field spans spatially from $-3.6 < X/D < 7.8$. Each vector map was post-processed using a two-step sequence: first, a validation routine examined a 5×5 vector area and replaced rejected vectors with an averaged estimate; second, an averaging filter was applied to each 5×5 vector area to reduce noise. The rejection criterion was determined as a vector being more than 10% different in magnitude than the surrounding vectors average. An invalid vector is one that does not accurately capture the velocity information at a point in the flow field. Vectors meeting the above criteria were replaced by the mean of their neighbors.

An ensemble of 200 sequential snapshots was acquired and a similar POD and estimation process as undertaken with the CFD data was repeated for each of the sensor configurations. The uncertainty of the PIV velocity measurements was estimated to be about 7–8% of the freestream velocity, based on the laser timing and displacement of the particles between snapshots. From Fig. 6, it can be seen that the sensor configuration, detailed in Table 2, brings the RMS of the

estimation error to 5–6% for the first two modes and to about 20% of modes 3–4. This error should be acceptable for a moderately robust controller. For the uncertainty in the velocity measurement error of 7–8%, it seems that the above results, especially for modes 1–2, are fairly accurate. It is important to note that the design of the sensor number and placement is based on measurements based on CFD data. This design is verified using measurements from experiments. The experimental data, based on PIV measurements, is inherently noisy. This noise has not been isolated and modeled into the linear stochastic estimator used in this effort. Therefore, given the approach pursued, the measurement error does have an effect on the quality of the mode amplitude estimates.

The velocity signals, provided by a certain configuration of sensors, are first used for calculation of the vorticity and then processed by the estimator to provide the estimates of the first 4 modes. The estimation scheme, based on the linear stochastic estimation procedure, predicts the temporal amplitudes of the first 4 POD modes from a finite set of measurements obtained from CFD/experimental data. The coefficients C_s^n in Eq. (4) are obtained via the linear stochastic estimation method from the set of discrete snapshots (200 for experiments and 70 for CFD simulation). This procedure is done off-line just once for each case.

Recently, Wilcox [29] introduced a sensor placement and number method for the same problem dealt with in this paper using a ''gappy'' POD procedure, which is the extension of the POD method that allows the consideration of incomplete data sets. The data set used by Wilcox [29] was identical to the one used in this effort. Even though the sensor placement was different for both approaches, the estimation errors are about the same. However, the heuristic approach, developed in this effort, requires less computation for the same level of performance.

The sensor placement approach presented in this paper is an important building block on the path towards closing the loop. The closed-loop control approach developed by Cohen et al. [30] is closely connected with the well documented lock-in phenomena, whereby the vortex shedding frequency aligns itself with that of the exciting force. Lock-in has been observed from Reynolds numbers of less than a hundred up to a few hundred thousands. As a result of the above phenomenon, the flow behaves in a two-dimensional fashion. When the low-dimensional POD model is based on snapshots from the lock-in regime, there is reason to believe that the proposed method of sensor placement will be valid. This hypothesis, while making a lot of sense, has yet to be proven. The section containing the results and discussion has been modified to include the above argument.

7. Conclusions and recommendations

A heuristic procedure was developed to determine the placement and number of sensors for the feedback control suppression of the wake instability behind a circular cylinder. This procedure is based on a low-dimensional, proper orthogonal decomposition modeling and linear stochastic estimation. The development of the procedure was based on COBALT CFD simulations of a cylinder at a Reynolds number of 100. Experimental studies, based on noisy experimental data obtained from the water tunnel cylinder model at a Reynolds number of 108, validated the effectiveness of the developed sensor placement and design procedure. Results show that for experimental data, the root mean square estimation error of the estimates of the first 2 modes

was within 6% and for the next 2 modes was within 20%. This level of error is acceptable for a moderately robust controller like the one developed by Cohen et al. [25].

Further research will aim at refining the developed heuristic procedure for sensor number and placement by taking symmetry, with respect to the x-axis, into account. In this effort, we noticed the potential for estimation error improvement by placing sensors at maxima/minima of the spatial eigenfunctions of modes 1–4. This potential should be further examined in a sensitivity study. Furthermore, there may be additional cost improvements to be gained by implementing a non-linear estimator instead of the linear stochastic estimator. It will be beneficial to examine the generic nature of the developed strategy for different bluff body geometries and Reynolds numbers.

It is interesting to note that recently published results by the USAFA team [31] for a "D" shaped cylinder at $Re = 350$ show that using the sensor placement method developed in this current effort, surface mounted pressure sensors provide accurate estimates of the wake flow field pressure and velocity POD mode amplitudes. Furthermore, it appears that as long as the frequencies picked up by the measurements (whether surface mounted or non-intrusive flow-field velocity components) correlate to the basic frequency composition of the POD reduced order model (based on vorticity, velocity components or pressure) the proposed sensor placement and number strategy is effective. Once the frequency content is picked up cleanly, and this is a necessary condition, then the LSE basically enables the calculation of the scaling factors. For the data used, both numerically obtained from direct Navier–Stokes simulations and experimentally collected form the water tunnel PIV measurements, we find that the LSE is effective. At this point, it is important to take a look at the point of view of a real-life application.

The current research effort on closed-loop control of the von Kármán wake instabilities have addressed the issue of sensor placement and number based on non-intrusive sensors in the wake. This approach may not always be implemented and it is important to develop an effective method for sensor placement and number based on body mounted sensors. These sensors may measure skin friction or surface pressures, as done in this effort. The advantages of surface mounted sensors are

- simple, relatively inexpensive and reliable,
- essential for real-life, closed-loop flow control applications where the direct measurement of the wake flow field is cumbersome (if not impossible),
- enable "nearly collocated" sensors and actuators, which eliminates substantial phase changes (affects controller design).

For real-life applications, an array of skin friction sensors can easily be integrated. The introduction of surface mounted skin-friction sensors would enable direct measurement of the vorticity on the surface. Therefore, a POD model based on vorticity is a promising candidate for closed-loop control. The final concern is whether the proposed method is effective. It is based on heuristics and no mathematical proof of its optimality has been attempted. To this end, we would like to mention recent results published by Willcox [32]. A "gappy" POD method was introduced that allows the consideration of incomplete data sets. An optimization formulation was developed and results were compared to those presented in this paper based on the same data sets. It was found, for the cylinder wake problem at $Re = 100$, the heuristic procedure developed in this method provided more accurate estimates.

Acknowledgment

The first author would like to acknowledge the support provided by the AFOSR/ESEP program. The authors would like to acknowledge the support and assistance provided by Dr. Belinda King (AFOSR), Lt. Col. Sharon Heise (AFOSR) and Dr. James Myatt (AFRL). The authors would like to thank cadets John Dayton and Kevin Hoy for collecting the experimental data in the water tunnel and Major Jim Forsythe for providing the CFD model.

References

[1] Gillies EA. Low-dimensional control of the circular cylinder wake. J Fluid Mech 1998;371:157–78.
[2] von Kármán T. Aerodynamics: selected topics in light of their historic development. Ithaca, NY: Cornell University Press; 1954.
[3] Park DS, Ladd DM, Hendricks EW. Feedback control of a global mode in spatially developing flows. Phys Lett A 1993;182:244–8.
[4] Roussopoulos K. Feedback control of vortex shedding at low Reynolds numbers. J Fluid Mech 1993;248:267–96.
[5] Williamson CHK. Vortex dynamics in the cylinder wake. Ann Rev Fluid Mech 1996;8:477–539.
[6] He JW, Glowinski R, Metcalfe R, Nordlander A, Periaux J. Active control and drag optimization for flow past a circular cylinder. J Comp Phys 2000;163:83–117.
[7] Li F, Aubry N. Feedback control of a flow past a cylinder via transverse motion. Phys Fluids 2003;41(8): 2163–76.
[8] Abergel F, Temam R. On some control problems in fluid mechanics. Theor Comput Fluid Dyn 1990;1:303–25.
[9] Li Z, Navon IM, Hussaini MY, LeDimet FX. Optimal control of cylinder wakes via suction and blowing. Comput Fluids 2003;32:149–71.
[10] Homescu C, Navon IM, Li Z. Suppression of vortex shedding for flow around a circular cylinder using optimal control. Int J Num Meth Fluids 2002;38(1):43–69.
[11] Holmes P, Lumley JL, Berkooz G. Turbulence, coherent structures, dynamical systems and symmetry. Cambridge: Cambridge University Press; 1996.
[12] Sirovich L. Turbulence and the dynamics of coherent structures. Part I: Coherent structures. Quart Appl Mathemat 1987;45(3):561–71.
[13] Balas MJ. Active control of flexible systems. J Optimizat Theory Appl 1978;25(3):217–36.
[14] Meirovitch L. Dynamics and control of structures. New York: John Wiley & Sons, Inc.; 1990.
[15] Adrian RJ. On the role of conditional averages in turbulence theory. In: Zakin J, Patterson G. (Eds.), Proceedings of the Fourth Biennial Symposium on Turbulence in Liquids. Princeton: Science Press, 1977.
[16] Cohen K, Siegel S, McLaughlin T, Myatt J. Proper orthogonal decomposition modeling of a controlled Ginzburg–Landau cylinder wake model. In Proceedings of 40th Aerospace Sciences Meeting and Exhibit, Reno NV 2003; AIAA Paper 2003-1292.
[17] Baruh H, Choe K. Sensor placement in structural control. J Guidance Cont 1990;13(3):524–33.
[18] Lim KB. A disturbance rejection approach to actuator and sensor placement. NASA CR-201623, January–February, 1997.
[19] Cobalt CFD, Cobalt Solutions, LLC, URL: http://www.cobaltcfd.com [cited 14 February 2003].
[20] Oertel Jr H. Wakes behind blunt bodies. Ann Rev Fluid Mech 1990;22:539–64.
[21] Panton RL. Incompressible flow. 2nd ed. New York: John Wiley & Sons; 1996.
[22] Min C, Choi H. Suboptimal feedback control of vortex shedding at low Reynolds numbers. J Fluid Mech 1999;401:123–56.
[23] Smith DR, Siegel S, McLaughlin T. Modeling of the wake behind a circular cylinder undergoing rotational oscillation. AIAA Paper 2002–3066, June 2002.
[24] Cameron J, Sick A, Cohen K, Wetlesen D. Siegel S. Determination of an effective densor configuration for suppression of the von Karman vortex street. AIAA Paper 2004–0578, January 2004.

[25] Cohen K, Siegel S, McLaughlin T, Gillies E. Feedback control of a cylinder wake low-dimensional model. AIAA J 2003;41(7):1389–91.
[26] Siegel S, Cohen K, McLaughlin T, Myatt J. Real-time particle image velocimetry for closed-loop flow control studies. In: Proceedings of 40th Aerospace Sciences Meeting and Exhibit, Reno NV 2003; AIAA Paper 2003-0920.
[27] Bayon de Noyer. Tail buffet alleviation of high performance twin tail aircraft using offset piezoceramic stack actuators and acceleration feedback control. Ph.D. Thesis, Aerospace Engineering, Georgia Institute of Technology, Atlanta, Georgia 30332, November 1999.
[28] Freeman RA, Kokotoviæ PA. Robust nonlinear control design–state space and Lyapunov techniques. Boston: Birkhäuser; 1996. 1–13.
[29] Willcox K. Unsteady flow sensing and estimation via the gappy proper orthogonal decomposition. In: Peraire J. Khoo BC, editor. Proceedings of SMA Symposium on High Performance Computation for Engineered Systems (HPCES), January 2004.
[30] Cohen K, Siegel S, McLaughlin T. Control issues in reduced-order feedback flow control. In: Proceedings of 42nd Aerospace Sciences Meeting and Exhibit, AIAA Paper 2004-0575.
[31] Cohen KD, Siegel S, Luchtenburg M, McLaughlin T, Seifert A. Sensor placement for closed-loop flow control of a 'D' shaped cylinder wake. Invited Session, 2nd AIAA Flow Control Conference, 28 June–1 July 2004, Portland, Oregon, AIAA-2004-2523.
[32] Willcox K. Unsteady flow sensing and estimation via the Gappy proper orthogonal decomposition. 34th Fluid Dynamics Conference and Exhibit, 28 June–1 July 2004, Portland, Oregon, AIAA-2004-2415.